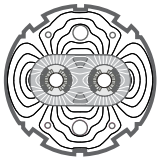

LHC Project Note draft

April 14, 2002

Simulation of the LHC Long-Range Beam-Beam Effect at the SPS

J.-P. Koutchouk, G. de Rijk, F. Zimmermann

Keywords: beam-beam

Summary

1 Motivation and principle of the SPS Experiment

The long-range beam-beam effect has been identified as being the primary limit of the LHC performance. Tracking and analysis of the diffusion of the action (amplitude) [1] seem to show that, at the nominal performance level, the single particle motion becomes unstable at amplitudes above 5.5σ. The onset of chaos in more recent studies [2] gives an even lower threshold around 4σ. It is doubtful that a dynamic aperture as small as this is acceptable in terms of beam lifetime.

A correction system was proposed to cancel the long-range beam-beam effect [3]. It is based on simulating the integrated long-range beam-beam kicks experienced by the beam using a wire corrector running along each beam. The sign and intensity of the electric current traversing the wire is adjusted to compensate the long-range beam-beam kicks. By satisfying optical conditions on the locality of the correction, it is possible to cancel exactly the perturbation. In practice, due a spread of the beam aspect ratio at the long range interaction points, the correction is accurate over about 10 orders in the multipolar expansion of the perturbing field. It was shown both by the tune footprint [3] and the diffusion of the action [4] that the correction cancels the effect of the beam-beam kicks very efficiently.

This accuracy opens the possibility of simulating in the SPS the beam dynamics under the influence of the long-range beam-beam kicks. A scaled version of the beam-beam compensator can be used to excite the effect rather than to correct it.

Given the betatron phase advance in the high-luminosity LHC insertions, the long-range beam-beam kicks in a single LHC insertion can be lumped and the simulation by a single wire excitor is accurate. The phase shift between the 2 LHC high-luminosity insertions cannot be simply simulated in the SPS, using a single wire. Rather a worst case where the effects of the 2 insertions are additive is considered. Dedicated tracking studies are needed to predict the beam behaviour in these conditions and compare it with the nominal LHC situation.

If this experiment confirms that the long-range beam-beam interactions are indeed dangerous for the beam, an extension of the setup can be interesting to investigate the efficiency of the compensation. In order to provide credible clues (in the SPS a wire compensates another wire), the compensator must be installed with an error in the betatron phase advance similar to that in LHC. The excitor (or beam) must be movable to simulate a situation where the beam-beam and beam-wire distances can be different. For amplitudes up to 7 sigma, the simulation at the SPS should be realistic and allow the study of the efficiency and robustness of the scheme.

2 Scaling the Beam-Beam Compensation to the SPS Energy

The critical field of a wire is given by

$$B_c = \frac{\mu_0 \, I_b}{2\pi r_c} \tag{1}$$

where I_b is the LHC beam current and $r_c = (n_0 - a)\sigma_b$ the separation between the center of the excitor beam and the position of the oscillating particle of the weak beam at the limit of stability. The average beam separation is $n_0 = 9.5$. From [1], $a \approx 5.5$. The corresponding kick received by the critical particle is

$$\theta_c = \frac{B \, l_{eff}}{B\rho} = \frac{1}{B\rho} \, \frac{\mu_0}{2\pi} \, \frac{I_b \, l_{eff}}{(n_0 - a)\sigma_b} \tag{2}$$

Let us express the energy dependence of the beam size:

$$\sigma_b = \sqrt{\beta \, \frac{\epsilon_n}{\gamma}} \tag{3}$$

where ϵ_n is the normalized emittance.

The scaling law versus energy is not straightforward as it depends both on the beam rigidity and the beam-wire separation. Ideally, we wish to keep the problem invariant when the beam energy is changed but the beam separation is kept constant when expressed in beam σ. The quantity of interest is then the maximum of the perturbation $\Delta x(s)$ normalized by the beam size:

$$\frac{\Delta x(s)}{\sigma(s)} = \frac{\sqrt{\beta(s)}}{\sigma(s)} \sqrt{\beta} \, \theta_c = \frac{1}{\epsilon_n} \, \frac{\gamma}{B\rho} \, \frac{\mu_0}{2\pi} \, \frac{I_b \, l_{eff}}{(n_0 - a)} \tag{4}$$

The relative perturbation does not depend on the energy neither on the β-function. This non-intuitive result is confirmed by simulation [5].

3 Principle of the SPS BBLR

The simulator of the strong beam must be strong enough to kick the SPS beam as if all the LHC long range interactions would take place at the same machine azimuth. Given the

invariance of the perturbation with the energy, the integrated kick shall be the same as that of LHC for the same normalized emittance. In order to reduce the intensity required in the BBLR, we shall consider three cases:

- a reference case with the nominal LHC emittance and the nominal current in the BBLR,
- a case with the SPS emittance reduced by a factor 3, either directly from the PS (commissioning beam) or beam scraping in the SPS; the BBLR current is then reduced by the same factor,
- a case with three parallel wires instead of one; the BBLR current may be further reduced.

.

The BBLR must be placed at a position where the SPS beam has the same aspect ratio as the LHC beam when it suffers long-range interactions, i.e. about round beams.

In order to minimize the cost and the preparation time of the experiment, the BBLR and its powering will be made of recuperated and transformed existing equipment. For the same reason, the BBLR excitor will not be movable but rather fixed. Instead, the beam will be moved towards the excitor to study the dependence of the perturbation versus the beam-beam separation. This creates two kinds of constraints:

- aperture issues for normal operation,
- a constraint on the maximum energy at which to carry out the experiment: the bumping capability of the SPS orbit correctors are indeed quite limited.

These issues will be addressed in the following sections.

4 Geometrical Parameters of the Beam-Beam Excitor BBLR

4.1 Implementation

The BBLR is implemented by modifying two existing long couplers of type BCPL. On each BCPL, two opposing coupler antennas are suppressed to leave the space for the BBLR excitor and its feedthroughs. In this way, by using the four remaining antennas of the two BCPL's, it remains possible to measure the orbit at the position of the BBLR while leaving the space for the excitor busbar. The latter will be positioned in the low position of the vertical plane. This is felt safer to minimize the probability of damage to the BBLR or interference with the SPS aperture in case of a deformation or break-down of the BBLR components.

4.2 Geometry

The internal diameter of the BCPL is smaller than that of the vacuum chamber (156 mm, see table 1). The contribution to the impedance is estimated to be negligible (agreed with P. Collier 22/2/02).

Parameter	value	unit
Number of modules	2	
mechanical length per module	710	mm
electrical length per module	600	mm
diameter of vac. chamber	133	mm
diameter of beam aperture (without excitor busbar)	115	mm
position of the antennas	45	degree

Table 1: Geometrical parameters at the BBLR's

4.3 Azimuth of the Experiment

The criterion is to find a place where the beam is approximately round to simulate an LHC beam at the IP. A compromise is made in such a way that another nearby position is available for a future compensation of the beam-beam effect (BBLRC) with the proper phase shift between BBLR and BBLRC and approximately round beams as well.

The position between QD517 and QF518 is selected: Assuming a normalized emittance

Position	azimuth m	SPS position	β_x m	β_y m	D_x m
BBLR1	5168.173	51760	45.99	51.45	-.30
BBLR2	5168.983	51771	48.27	49.07	-.31

Table 2: Optics parameters at the BBLR's

of 1.4 10^{-6} (1 sigma) and a momentum spread of 0.001 at 26 GeV (1 sigma), the effect of the dispersion is negligible. The beams are round to about +- 1.5 %.

4.4 Machine Aperture and Transverse Position of the BBLR Excitor

4.4.1 Requirements

The first requirement for the BBLR excitor is not to limit the machine aperture for normal SPS operation. While this criterion is well defined for a perfect machine, some safety margin must be allowed for local deformation of the orbit or local misalignments. This safety margin must not be taken too large for the following reasons:

- an orbit bump is necessary to adjust the beam-excitor separation in a range of 4.5 to 12 σ. This should not exceed the capability of the SPS orbit correctors which are quite limited,
- within the extent of this bump, the BBLR excitor must remain the aperture limit,
- at injection energy, the natural beam lifetime may not be sufficient to carry out the experiment in the best conditions; increasing the energy further pushes the demand on the orbit correctors,

- to maximize the efficiency of the SPS studies, the experiments requiring coasting beams should share the same machine cycle. One experiment requires 60 GeV to 80 GeV while another presently prefers 80 GeV.

4.4.2 Aperture Implementation in MAD

The MAD program was tweaked to allow for aperture calculations including the required deformations of the closed orbit. This was achieved by defining and installing aperture elements upstream and downstream of the bends, quadrupoles and known aperture limits (TID's). The aperture elements are dummy RBENDS of zero length and angle where the angles and curvatures of the entry faces are taken for the +X, -X, +Y, -Y coordinates of the geometrical aperture. This opens the possibility of calculating the geometrical aperture taking into account orbit bumps, a momentum offset and the actual beam size including possible focusing imperfections. The definition of the aperture is the same as that used by G. Arduini (except for an orbit deviation) and the input data are identical. In identical situation (nominal optics), the MAD program was checked to yield the same result as already calculated by G. Arduini.

4.4.3 BBLR Transverse Position and Machine Aperture

For the worst beam parameters (momentum of 26 GeV/c, normalized emittance of 13.8 10^{-6} m.rad), the SPS aperture is given on figure 1. The internal dump TIDV limits the vertical aperture to 3.04 σ at one point in the machine. In the shadow of the TIDV, the bending magnets produce a quasi continuous second aperture limit at 3.39 σ. At the position of the BBLR, the beam σ is 5.0 mm.

To be safe and insensitive to closed orbit deviations, we specify that the BBLR should be in the **shadow of the second aperture limit**. Eventhough the second aperture limit is distributed all along the machine, a safety margin is taken to cope with a local orbit π-bump which would not propagate to the rest of the machine. It should be noted that the near-by half-cell is equipped with a dipole vacuum chamber. Depending over which cells the π-bump develops, it is likely that this chamber will limit first the aperture. For the other cases, we take an additional safety margin allowing a bump of 3 mm peak in the quadrupole.

These requirements yield a distance of 19 mm between the axis of the vacuum chamber and the edge of the BBLR excitor (figure 5). The detail of the aperture in the region of the BBLR is given on figure 2. The BBLR is at 5168 m. It is in the shadow of the aperture of the upstream half-cell and just sticking in as compared to an aperture restriction occurring 6 m before (vacuum experiment using a MBB chamber).

5 Bumping the Beam Towards the Beam-Beam Excitor

5.1 Range for the Beam-Wire Separation

The nominal average beam-beam separation in LHC is 9.5 σ. The critical kick which makes the motion unstable occurs at an amplitude of 5.5 σ, hence at a minimum separation of 4

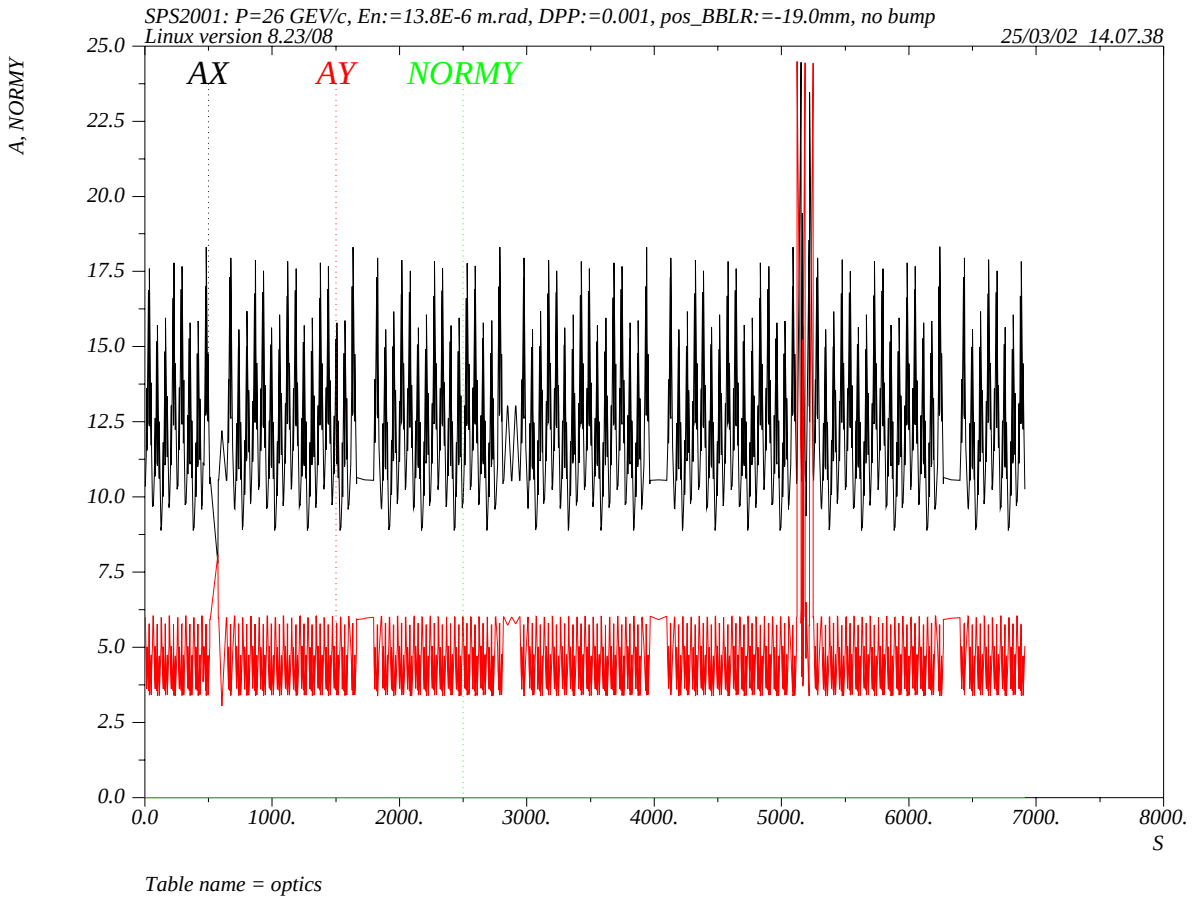

Figure 1: SPS aperture (A_x, A_y) in the worst case

σ. It is interesting to be able to reduce the average separation to 4 σ, where the complete beam should experience critical kicks. Due to the finite diameter of the wire representing the strong beam (about 2 σ), it seems reasonable in practice to be able to decrease the separation to 4.5 σ, leaving a clearance of 3.5 σ for the beam oscillations. When calculating the bumps required for a separation of 4.5 σ, due account should be taken of the possibility of running the SPS with an emittance reduced by a factor of 3 as compared to the nominal LHC normalized emittance.

The largest beam-wire separation should be about 12 σ as it is foreseen to be actually used in LHC.

5.2 Scenarios, kick strength and aperture

The scenarios considered are summarized in table 3 and discussed below. The separation types are: 1 for a π-bump, 3 for the superposition of a π-bump and a 3π-bump, 5 for the

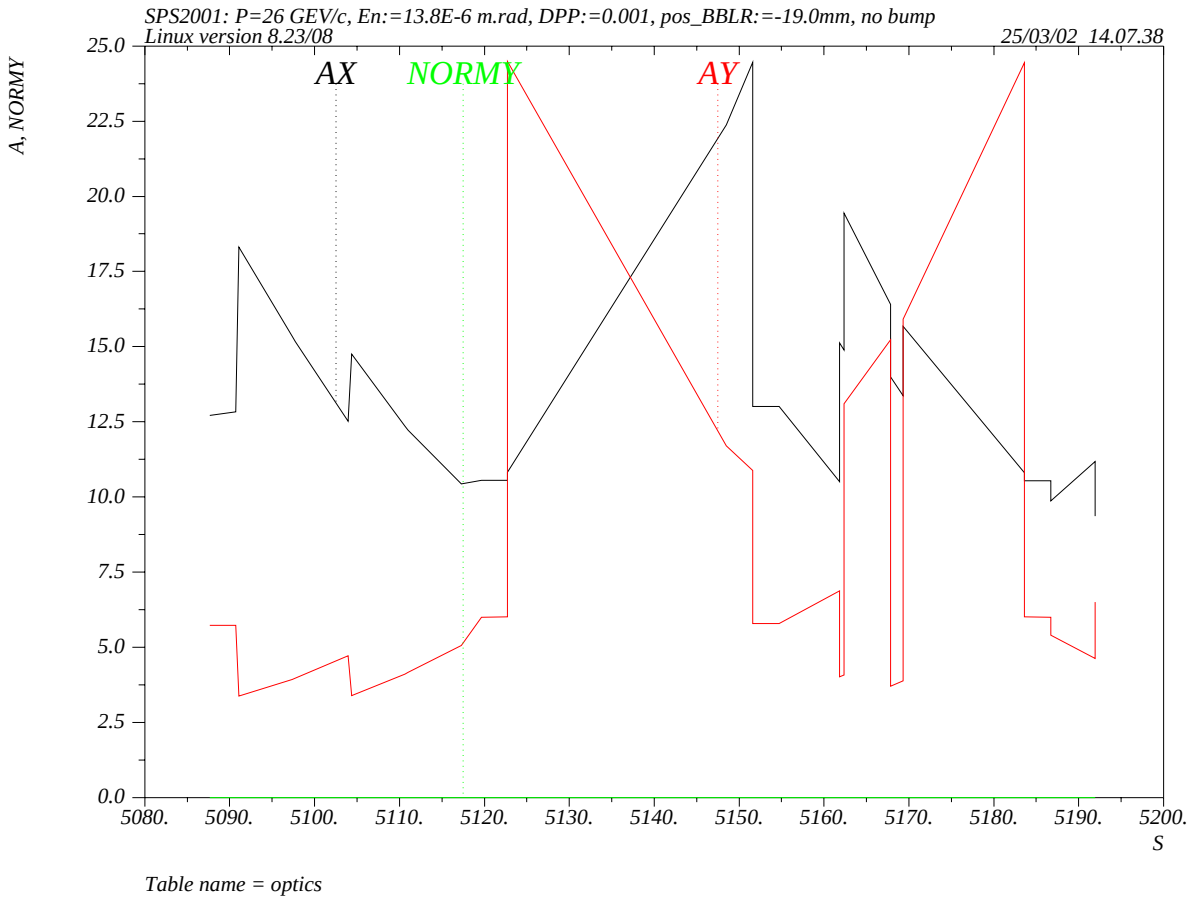

Figure 2: Detail of the SPS aperture in the vicinity of the BBLR (worst case). The BBLR is at 5168 m.

superposition of a π-bump, a 3π-bump and a 5π-bump. If a bump saturates, it is set to its maximum and complemented by another bump. The kicker strength quoted is that of the bump which does not saturate. The aperture limit named 'near-by" is the MBB chamber a few meters upstream of the BBLR. The diameter of the BBLR excitor wire is assumed to be 2 mm.

5.2.1 Case 1: 26 GeV/c, Nominal Emittance

This is the simplest scenario for the machine study. The most serious constraint is the limitation of the maximum amplitude by the TIDV at 6.5 σ. This should however be just enough to observe the phenomenon. The beam-wire separation can be reduced without limitation to enhance the diffusion. Larger separations are limited to 10.6 σ by the aperture within the bump. Given the TIDV aperture limit, large separations do not seem especially interesting.

	separation			aperture			
Case	Δ	type	kick	TIDV	Bends	Near-by	BBLR
	σ		%	σ	σ	σ	σ
1	no bump: 8.4	-	0%	6.5	7.3	8.6	8.0
26 GeV/c	9.5	1	16.2			7.7	8.9
$\epsilon = 3.0\ 10^{-6}$	4.5	1	72.3			4.5	3.9
	10.6	1	35.7			6.6	10.0
2	no bump: 12.2	-	0	9.6	10.7	12.6	11.7
26 GeV/c	9.5	1	37.0			9.5	8.6
$\epsilon = 1.4\ 10^{-6}$	4.5	1	97.5			4.4	3.6
	12.0	1	6.9			12.1	11.1
3	no bump: 12.2	-	0	9.5	10.6	12.6	11.6
55 GeV/c	9.5	1	76.9			9.5	8.6
$\epsilon = 3.0\ 10^{-6}$	4.5	1	206			4.4	3.6
	12.0	1	12.6			12.1	11.1
4	no bump: 17.8	-	0	13.9	15.5	18.4	17.0
55 GeV/c	9.5	3	55.1			9.4	8.1
$\epsilon = 1.4\ 10^{-6}$	4.5	5	31			4.2	3.1
	12.0	3	10.6			12.0	10.7

Table 3: Scenarios fo the machine study

5.2.2 Case 2: 26 GeV/c, Reduced Emittance

The emittance is reduced to push the TIDV aperture to the nominal beam-wire separation of 9.5 σ. The required normalized emittance becomes $\epsilon = 1.4\ 10^{-6}$ m.rad. It may be obtained either from the PS (commissioning beam) or by scraping. A distinct advantage of this scenario is to reduce the requirement on the current flowing in the excitor wire by the ratio of the emittances, i.e. a factor 2.7.

If the beam lifetime is long at 26 GeV/c, this scenario is the most favourable. There are no limitations. The apparently large excitation of the orbit correctors may be reduced by at least a factor of two by superposing 3π and 5π bumps.

5.2.3 Case 3: 55 GeV/c, Nominal Emittance

In this scenario, the energy is adjusted to provide the required 9.5 σ aperture for the nominal normalized emittance. This scenario is equivalent to scenario 2 with the exception of a large overrun of the orbit corrector strength. This may be alleviated by using a superposition of π, 3π and 5π bumps. Figure 3 shows that the superposition of the three bumps does not create any other aperture limitation within the bump.

5.2.4 Case 4: 55 GeV/c, Reduced Emittance

Thanks to 5π bumps, it is possible to use this scenario with the advantage of an excitor current reduced by a factor 2.7.

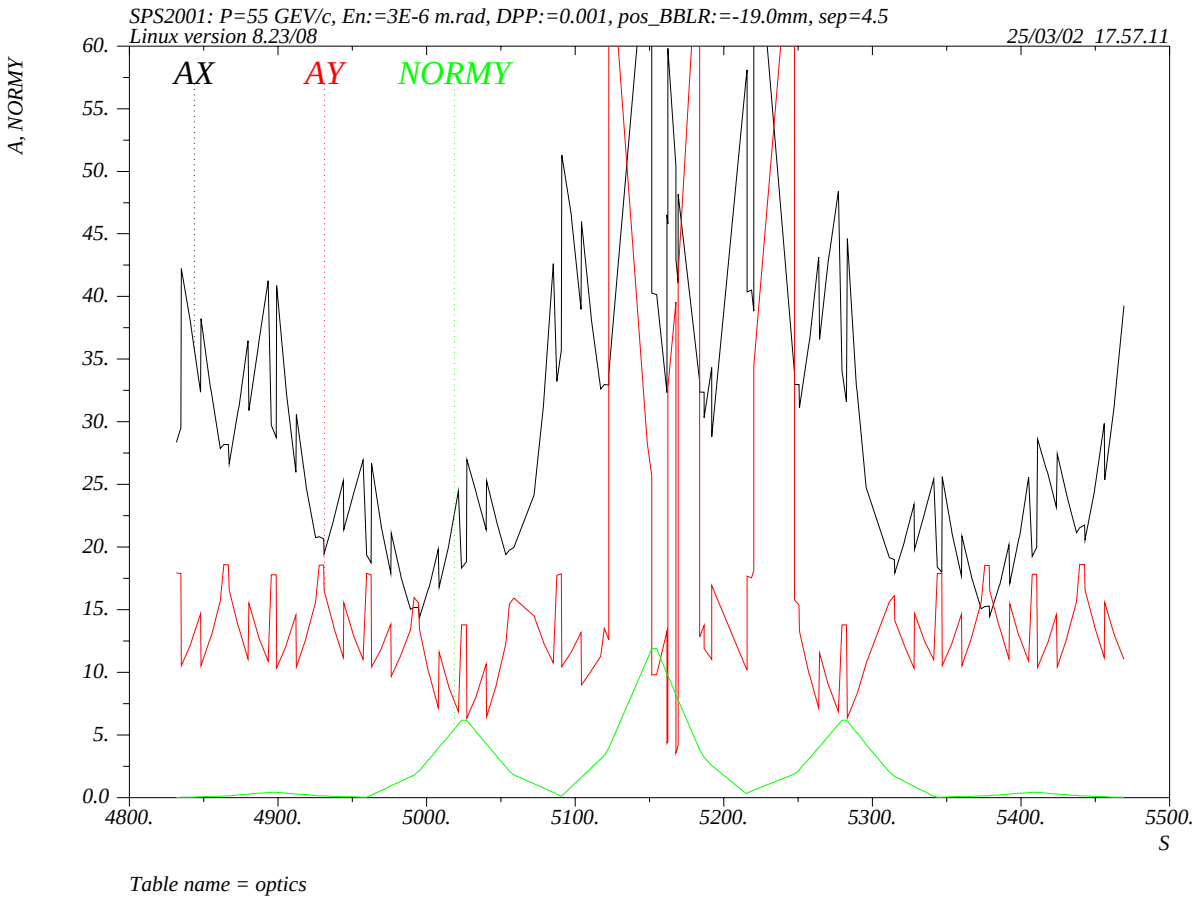

Figure 3: Aperture over the extent of the combined bumps for case 3 and a separation of 4.5 σ; NormY is the absolute value of the normalized orbit deviation

5.3 Conclusion

Several scenarios are possible, either at injection energy with a reduced beam emittance or around 55 GeV with either the nominal or a reduced emittance. It does not seem realistic to aim at an energy higher than 55 GeV, as the margin in the orbit correctors is small. At 60 GeV, there is almost no margin left. Some could be created by superposing a 7π or longer bumps. The maximum reachable energy will depend on the alignment accuracy of this machine section. At high energy with a reduced emittance, the physical size of the wire starts reducing the aperture available to the beam when the beam separation is small. This shows that the assumed diameter of 2 mm should not be increased significantly.

6 Electrical Parameters of the Beam-Beam Excitor BBLR

6.1 Intensity of the Current

Ideally, the integrated intensity shall be 320 A.m. With an effective length of 1.2 m, the intensity should be 267 A.

According to the scaling laws in section **??**, if the emittance is reduced by a factor of 2.7 as compared to LHC: 3.75 to 1.4 10^{-6} m.rad, the demand on the intensity is thereby reduced to 118.5 A.

6.2 Cross-section of the Wire

We have seen in section **??** that clearance necessary for large amplitude particles require a small wire diameter of the order of 2mm. Variations are possible if they are small compared to σ. We should consider its minimum value in the scenarios, equal to 0.65 mm.

6.3 Heating in an isolated conductor

We solve the Fourier equation in the simplified case of an isolated straight conductor where the heat is conducted to the extremities of the wire assumed to behave as heat-sinks. We neglect radiation, as the final aim is to design the system in such a way that it is negligible. The Fourier law is given by:

$$\vec{\phi} = -\lambda \overrightarrow{\text{grad}}\, T \tag{5}$$

ϕ is density of heat flux and λ the heat conductivity. The first principle of thermodynamics yields:

$$\rho_v c_p \frac{\partial T}{\partial t} = -\text{div}\vec{\phi} + q \tag{6}$$

q is the amount of heat per unit volume created inside the conductor, ρ_v the mass per unit volume per unit time and c_p is the heat capacity. We look for the steady-state solution obtained by combining Eq. 5 and Eq. 6:

$$\text{div}\lambda \overrightarrow{\text{grad}}\, T + q = 0 \tag{7}$$

We look for a design where the temperature increase remains modest. We may thus neglect the temperature variation of λ. In the 1D case, Eq. 7 becomes:

$$-\lambda \frac{\partial^2 T}{\partial x^2} + \left(\rho \frac{dx}{\pi r^2}\right) I^2 \left(\frac{1}{\pi r^2 dx}\right) = 0 \tag{8}$$

ρ is the electrical resistivity and r the radius of the wire. This equation is easily solved. The maximum temperature increase occurs at the mid-length of the wire and is given by:

$$\Delta T_{max} = \frac{1}{8\pi^2} \frac{\rho}{\lambda} \frac{L^2}{r^4} I^2 \tag{9}$$

where L is the length of the wire. The power dissipated in the wire is

$$P = \rho \frac{L}{\pi r^2} I^2 \tag{10}$$

The numerical values of the current density, power and temperature increase are given in table 5, assuming the physical parameters given in table 4. The wire would not resist the temperature increased and therefore must be cooled.

Material	ρ Ω.m	λ W/m.K
Cu	$1.70\ 10^{-8}$	390
Stainless steel		45
Al_2O_3	$< 10^{12}$	26-35
AlN	$< 10^{12}$	180

Table 4: Physical data for materials

Intensity A	Current density A/mm^2	Power W	ΔT degrees
10	3.2	0.32	19.9
20	6.4	1.3	79.5
50	15.9	8.1	497
100	31.8	32.5	1987
118.5	37.7	45.6	2791
150	47.7	73	4472
200	63.7	130	7950
267	85.0	231	14168
300	95.5	292	17890

Table 5: Temperature increase for the nominal wire conductor

6.4 Cooling by a Comb

The temperature increase is very large but the power involved is less than 250 watts. This leaves the impression that the wire can be cooled by passively conducting the heat outside the conductor. The most sensitive parameter in equation **??** is the length of the wire between two heat sinks. We can consider a support looking like a comb and imposing an external temperature periodically along the wire. Figure 4 shows the dependence of the temperature increase on the period of the cooling comb. For an efficient cooling(a safe temperature increase is about 80 degrees [N.Hilleret]), the period should be about 4 cm. In practice, this shows that the cooling should be done all along the length of the conductor by a continuous supporting structure.

6.5 Cooling by a Continuous Support

This solution assumes that the copper wire is brazed on a support. The support must be electrically isolated from the wire but thermically in excellent contact with it. At its other end, the support is in excellent contact with the stainless steel vacuum vessel, presumably

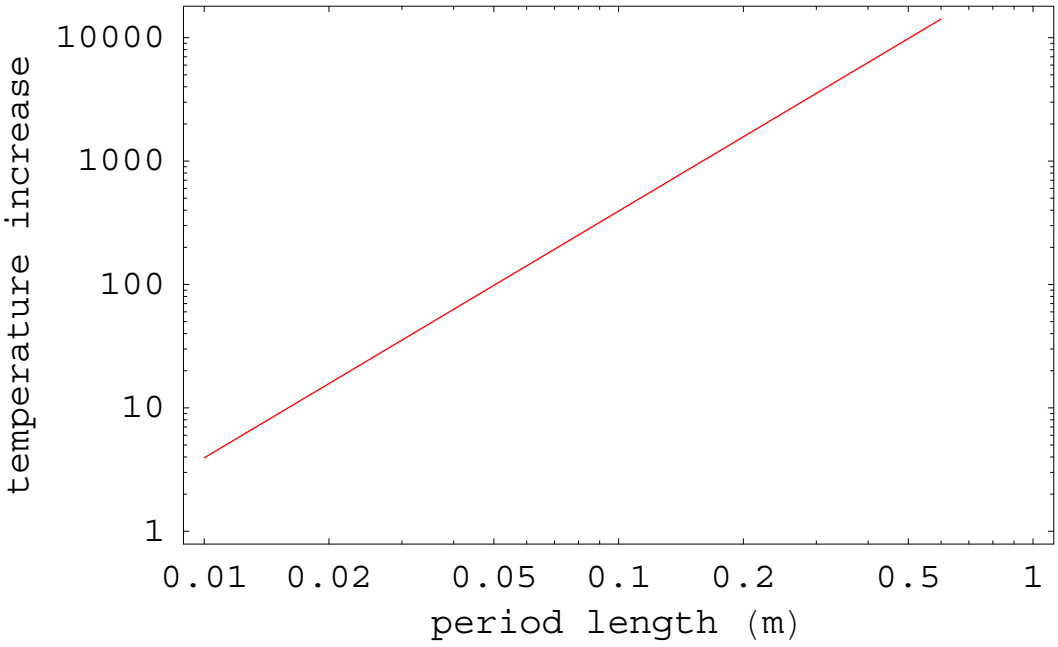

Figure 4: Dependence of the temperature increase on the period of the cooling comb

brazed on it. The schematic cross-section is shown on figure 5. We reduce again the heat transfer to a 1D problem, this time along the axis of the support as shown on figure 5. The solution is bound to be pessimistic, as the heat flux will escape away from this axis. We compute thus an upper bound for the temperature increase.

We assume that the contact between the wire and the support is effective over half of the circumference of the wire where the equipotentials of the heat flux deviate weakly from planes. This is again pessimistic as the final design can be extended to the whole circumference with curved heat flux lines. This however would un-necessarily complicate the calculation. At equilibrium, the wire conductor is at a fixed temperature $T_0 + \Delta T$, where T_0 is the temperature of the outside of the vacuum chamber. There is no generation of heat inside the cooling system made by the support and the chamber. The variation of the temperature along the support is therefore linear if the material is homogeneous.

6.5.1 Ideal case

We assume that the support is made of copper. A thin film of negligible heat resistance isolates electrically the wire from the support. The support itself is thermically connected to the outside, e.g. thru the feed-thrus, in such a way that the outside temperature is imposed at the outer extremity of the support.

The density of heat flux produced by the Joules effect flowing from the wire over half its circumference to the support is given by:

$$\phi = \rho \frac{dx}{\pi r^2} I^2 \frac{1}{\pi r dx} = \frac{1}{\pi^2} \frac{\rho I^2}{r^3} \tag{11}$$

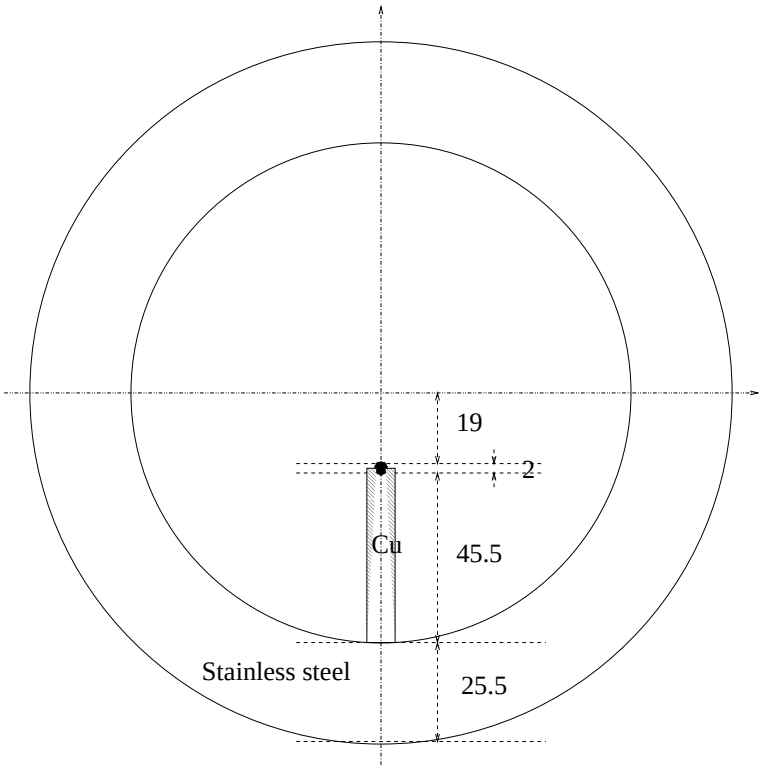

Figure 5: Schematic cross section of the BBLR used for thermal calculations

The Fourier law 5 yields the relation between the flux and the temperature gradient. If e is the height of the support, the flux density writes:

$$\phi = \frac{\lambda}{e}\,\Delta T \tag{12}$$

Let us solve equations 11 and 12 for ΔT:

$$\Delta T = \frac{\rho I^2}{\pi^2 r^3}\,\frac{e}{\lambda} \tag{13}$$

In this ideal case, the temperature increase is 22 degrees, i.e. negligible.

6.5.2 Support made of copper and stainless steel

This ideal case assumes that the heat is perfectly conducted outside of the vacuum vessel. We now consider the realistic case where the stainless steel vacuum bore is part of the cooling circuit, without a special high-conductivity circuit extracting the heat outside the chamber. This arrangement much simplifies the feed-thru's which need be only electrical. A simplified model assumes that the cooling circuit is made of 45.5 mm of copper (support) and 25.5 mm of stainless steel (chamber), with a perfect contact between both. Eq. 12 still holds provided e/λ is replaced by $\sum_i e_i/\lambda_i$:

$$\Delta T = \frac{\rho I^2}{\pi^2 r^3}\,\sum_i \frac{e_i}{\lambda_i} \tag{14}$$

The temperature rise becomes 84 degrees. This is just acceptable. This set up however does not take advantage of a free parameter, i.e. the thickness of the support. It can be made significantly larger than the projection of the contact surface between the wire and the support $\pi r = 3.14$ mm. A thickness of 6 mm would divide the density flux by 2 and the temperature increase accordingly. Using a T-shaped bar of copper would (45.5×45.5) would divide the flux density at the junction of the support and vacuum vessel by a factor of ten in such a way that the stainless steel conductivity would appear equal to that of the copper. It appears therefore that there is no need to conduct the heat to the outside, provided the support is largely dimensioned.

6.5.3 Electrical insulation between wire and support

For this calculation, we assume the solution proposed by N. Hilleret. The wire conductor is made of brasure Cu-Ag filling an Al_2O_3 tube of internal diameter 2mm and outer diameter 4mm (Goodfellow AL607080, page 420). If we compare to the ideal case, the temperature increase is 30 degrees instead of 22 degrees. The increase by 8 degrees due to the insulator appears rather negligible.

6.6 Conclusion

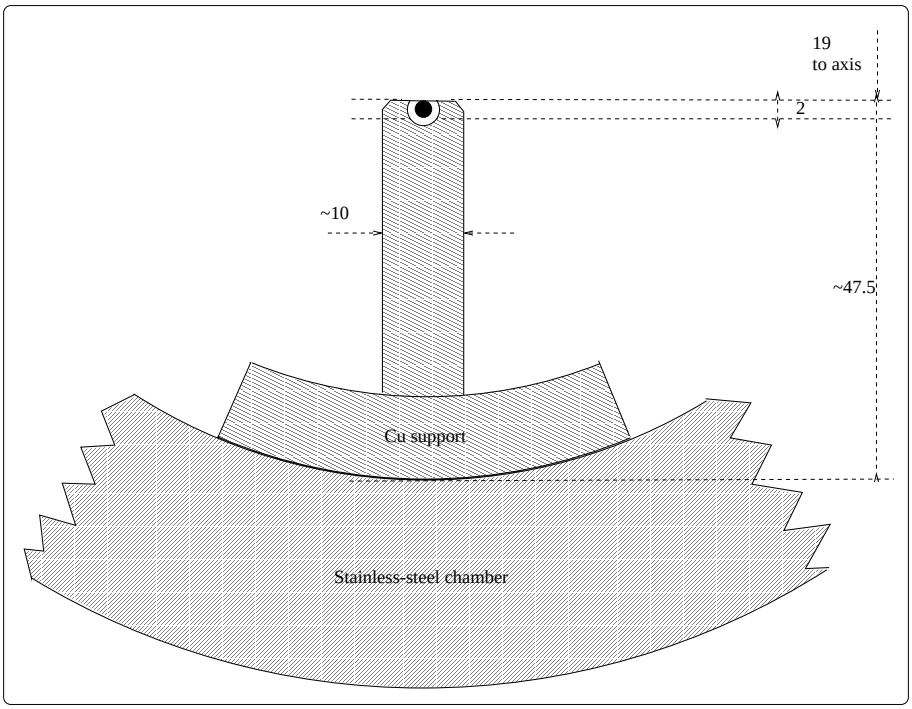

Figure 6: Schematic cross section of the BBLR in the BCPL

These simple calculations show that it must be possible to cool the wire corrector passively and without the need to conduct the heat outside of the vacuum vessel. The support should be continuous along the wire. Its thickness should be at least 6 mm, say 10 mm. The

support should be T-shaped such as to offer a large surface of contact with the stainless steel of the vacuum vessel. Dimensions 47.5 × 50 mm seem appropriate. The contacts between the wire, the support and the vacuum vessel should be excellent. This should be guarantied in this solution by brazing the copper wire inside the alumina tube, the alumina tube onto the copper support and the latter onto the stainless-steel vacuum chamber.

!+++
!+++

7 WHAT FOLLOWS IS TO BE REVISITED!!!!!!!!!!!!!

8 The Power Supply, the cables and the remote Control

The power supply and controls shall be installed in rack number: 1702 in BA5.

8.1 The Cables

- cables for the coupler giving the beam position (X and Y): cables available?? C. Boccard
- cable for powering the BBLR from BA5: a 4*94mm^2 Al cable has been recuperated by P. Woillet; it will be prolongated to the rack in BA5 and to the proper position in the tunnel. The extremities will be left without connectors for the moment. The order was passed by J. Koopman.
- control cable for setting the excitor current
- control cable for reading back the excitor current
- cable for the BLM (already available -¿ GianFranco)
- cable for the thermometer: J. Koopman found a spare cable from the tunel to BA5.

9 Required Beam Observables

- the beam-wire separation is a critical parameter; it will be measured with a short coupler to be installed adjacent to the wire excitor.
- the beam emittance; a normalized emittance down to 1E-6 mrad must be measurable with a reasonable accuracy (10 to 20%).
- the beam lifetime
- the beam loss rate at the wire excitor; a BLM will be installed downstream the wire corrector to monitor the losses during the experiment (unstable particles) and otherwise to verify that it does not become an aperture during normal operation. G. Ferioli

contacted 25/2/02: Test BLM's are available around this place. They are connected to the control room with a dedicated software. Monitoring on a 0.5 s period seems to be OK. At most, a small cable extension is to be foreseen. G.F. should be contacted when the BBLR tank is installed.

- the beam loss rate at a controlable aperture restriction (collimator) to measure diffusion a la Seidel.
- the wire current.
- (possibly) the wire temperature.

10 Operational and Safety Aspects

The vacuum chamber will be prepared now to receive this instrument hopefully during this shut-down. A 1 day machine stop is sufficient to exchange the instrument with the vac chamber section.

11 Budget

The budget line is: 96538
Expenditures:

- Cutting the vacuum chamber, putting flanges, etc... estimate (J. Camas) 3000SFr
- Cables: 60m * 10 Sfr 1000SFr
- Misc: 2000 SFr.

12 Summary of the SPS Beam and Machine Conditions

- mode: coast
- a single bunch is sufficient; more do not arm
- a reduced emittance from the PS or scraping down to the smallest normalized emittance: 1.2E-6 mrad assumed.
- any intensity with a naturally long lifetime
- energy: 26 GeV if the beam lifetime can be made larger than 1 hour, otherwise more. The lowest energy with a good lifetime is the best: the beam size is largest and the orbit corrector stronger. It is not sure that 80 GeV can be reached. - Assumed beam parameters (G. Arduini): * SPS 2001 optics * LHC beam: normalized emittance 1.2 E-6 (1 sigma) (reduced or scraped) momentum spread 0.001 (1 sigma) at 26 GeV

Acknowledgments

This project is a joint effort of: J. Camas, infrastructure, technical coordination, mechanical design, C.Boccard, J.P.Papis, J.Koopman for the coupler modification, instrumentation and cables, Thanks to J. Ramillon, P Woillet, G. Arduini, N. Hilleret, R.Jung for help and ideas,...

References

[1] Y. Papaphilippou & F. Zimmermann, "Weak-Strong Beam-Beam Simulations for the LHC", Proc. of the Workshop on Beam-Beam Effects in Large Hadron Colliders, CERN-SL-99-039, 1999.

[2] Y. Luo & F. Schmidt, "Weak-Strong Beam-Beam Tracking for LHC V6.0', in LHC Proj. Report 502, 2001.

[3] J.P. Koutchouk, "Correction of the Long-Range Beam-Beam Effect in the LHC using Electromagnetic Lenses", LHC Project Note 223, 2000.

[4] F. Zimmermann, "Weak-Strong Simulation Studies for the Long-Range Beam-beam Compensator", in LHC Proj. Report 502, 2001.

[5] F. Zimmermann, "Diffusive Aperture due to Long-range Collisions at Injection and Image-Charge Effects", LHC Proj. Note 250, 2001.